

NATIONAL AERONAUTICS AND SPACE ADMINISTRATION

Technical Report 32-1029

A Sensitive S-Band Noise Receiver Developed for the Mariner Mars 1964 Spacecraft Program

Louis H. Keeler  
Andrew J. Nalbandian  
Albert A. Olbeter

GPO PRICE \$ \_\_\_\_\_

CFSTI PRICE(S) \$ \_\_\_\_\_

Hard copy (HC) 3.00

Microfiche (MF) .65

ff 653 July 85

**N67 17824**

(ACCESSION NUMBER)

26

(PAGES)

CR-81637

(NASA CR OR TMX OR AD NUMBER)

(THRU)

(CO)

(CATEGORY)

FACILITY FORM 602

JET PROPULSION LABORATORY  
CALIFORNIA INSTITUTE OF TECHNOLOGY  
PASADENA, CALIFORNIA

November 15, 1966

NATIONAL AERONAUTICS AND SPACE ADMINISTRATION

*Technical Report 32-1029*

*A Sensitive S-Band Noise Receiver Developed  
for the Mariner Mars 1964 Spacecraft Program*

*Louis H. Keeler  
Andrew J. Nalbandian  
Albert A. Olbeter*

Approved by:



W. S. Shipley, Manager  
Environmental Requirements Section

JET PROPULSION LABORATORY  
CALIFORNIA INSTITUTE OF TECHNOLOGY  
PASADENA, CALIFORNIA

November 15, 1966

**TECHNICAL REPORT 32-1029**

Copyright © 1967  
Jet Propulsion Laboratory  
California Institute of Technology  
Prepared Under Contract No. NAS 7-100  
National Aeronautics & Space Administration

## **Acknowledgments**

The authors wish to acknowledge the work of Michael Gutierrez in the design and development of the S-band noise instrumentation. They also wish to express their appreciation for the generous support received from the JPL Telecommunications Division, especially from the following personnel: Harold Donnelly, Henry Paris, Jr., Charles Potts, Charles Stelzried, Charles Wakely, James Wilcher.

## Contents

<b>I. Introduction</b> . . . . .	1
<b>II. Spacecraft Telecommunications Subsystem and Requirement</b> . . . . .	1
<b>III. System Design</b> . . . . .	3
A. Receiver Sensitivity Considerations and Front End Design . . . . .	3
B. System Description . . . . .	3
1. Manual Scan Subsystem . . . . .	4
2. Predetection Record Subsystem . . . . .	4
C. S-Band Calibration Source . . . . .	5
<b>IV. System Calibration, Operation, and Performance Capabilities</b> . . . . .	5
A. System Packaging and Calibration . . . . .	5
B. System Operation and Performance Capabilities . . . . .	6
<b>V. S-Band Noise Receiver Operations Summary</b> . . . . .	6
A. Pasadena Operations Summary . . . . .	6
1. Noise Receiver Calibration . . . . .	7
2. Test Results . . . . .	7
3. Preparation for Cape Kennedy Tests . . . . .	8
B. Cape Kennedy Operations Summary . . . . .	9
1. Launch Complex No. 13 Test Configuration and Results . . . . .	9
2. Launch Complex No. 12 Test Configuration and Results . . . . .	9
3. Receiver System Calibration at Cape Kennedy . . . . .	9
<b>VI. System Design Improvements for Future Operational Requirements</b> . . . . .	10
A. Tunnel-Diode Amplifier . . . . .	10
B. Military Receiver R 390A/URR Motor-Driven Scan . . . . .	10
<b>Appendix A. Receiver System Noise Figure Measurements and Operation Procedure</b> . . . . .	11
<b>Appendix B. System Noise Temperature Analysis for Space Chamber Tests and High Bay Tests</b> . . . . .	14
<b>References</b> . . . . .	18

## Contents (contd)

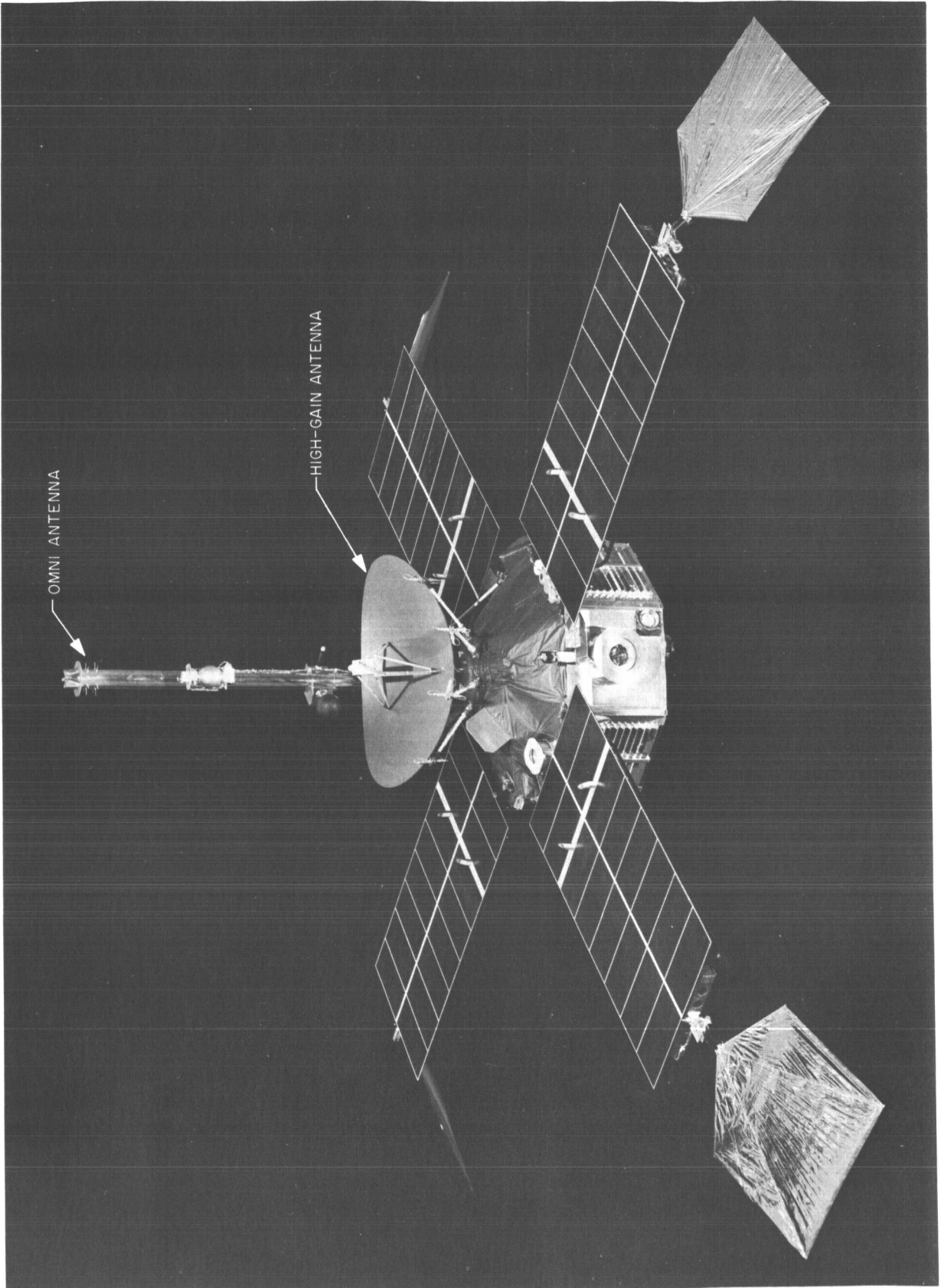
### Figures

1. Functional block diagram S-band Noise Receiver System . . . . .	2
2. Four networks in cascade . . . . .	3
3. S-band Noise Receiver System predetection record subsystem . . . . .	4
4. S-band Noise Receiver System CW calibration source . . . . .	5
5. S-band system packaging in consoles (in use at the AFETR) . . . . .	6
6. S-band Noise Receiver System input-output characteristic (manual system) . . . . .	7
7. EMI test equipment installation on MC-1, proof test model . . . . .	8
8. Functional diagram: MC-2 mission test . . . . .	8
9. Functional diagram: MC-3 and MC-4 mission tests . . . . .	8
A-1. S-band Noise Receiver System calibrator power output curve . . . . .	11
A-2. Noise figure measurement using Method II . . . . .	12
B-1. Space chamber test configuration . . . . .	14
B-2. Spacecraft Assembly Facility test configuration . . . . .	15
B-3. High bay omni antenna noise temperature measurement test configuration . . . . .	17

## Abstract

A sensitive S-band noise receiver was required for the *Mariner* Mars 1964 spacecraft program to verify spacecraft subsystems compatibility with the telecommunications subsystem. The basic problem was to design a readily portable, high resolution, low noise receiver system having a sensitivity approaching that of the permissible noise level for *Mariner* Mars spacecraft, and with a broad tuning range. A receiver utilizing a parametric amplifier and modified spacecraft transponder designs and modules was developed by the Electromagnetic Interference (EMI) Group. Predetection recording was incorporated along with a manual scan subsystem. It was determined that the noise receiver system permitted measurements as low as  $-151$  dbm in a 100 Hz bandwidth. The Receiver System and stable calibration source designs are discussed.

The Noise Receiver tests during *Mariner* spacecraft test operations at the Jet Propulsion Laboratory (JPL) Pasadena and at the Air Force Eastern Test Range (AFETR) Cape Kennedy are summarized below. The Noise Receiver System performed reliably and accurately. No major compatibility problems were encountered. The system verified that undesirable noise levels or spectral components were not present in the critical frequency regions and provided standby support for crucial tests during Pasadena and Cape Kennedy spacecraft operations. Some system design improvements for future spacecraft operational support requirements are discussed. The Receiver System noise-figure measurements and operation procedure employed are documented in Appendix A. The system noise temperature analysis for space chamber tests and high bay tests (Pasadena operations) are given in Appendix B.



Mariner Mars 1964 spacecraft



# A Sensitive S-Band Noise Receiver Developed for the *Mariner Mars 1964* Spacecraft Program

## I. Introduction

In deep space probes, with long-distance communications as a requirement, an extremely sensitive spacecraft receiver is a necessity. It is imperative that the spacecraft subsystems be compatible with the telecommunications subsystem. Any source of interference producing noise and/or a coherent signal in the region of the receive frequency might cause degradation of system performance and possibly abort a spacecraft mission. It is necessary to have a means of verifying, through a series of measurements, that the spacecraft receivers will not be degraded by RF noise contributed either by the spacecraft assemblies or by operational environments.

Since commercially available electromagnetic interference (EMI) equipment does not approach the sensitivities and resolutions required, the development of a sensitive S-band receiver system for the *Mariner Mars 1964* and future spacecraft programs was undertaken. The effort utilized the experience gained in the development and use of the *Ranger* L-band noise meter, which was employed as a principal tool for investigating crucial spacecraft lunar survival capsule/transponder, and spacecraft television/transponder compatibility problems (Ref. 1). This paper presents the particular test

requirements, the instrumentation developed, its calibration, operation, and performance.

## II. Spacecraft Telecommunications Subsystem and Requirement

The *Mariner Mars 1964* spacecraft telecommunications subsystem consists of: (1) an extremely narrow-band double superheterodyne, automatic phase tracking receiver operating at various frequencies in the neighborhood of 2115 MHz and (2) an integrally related transmitter with corresponding frequencies in the neighborhood of 2295 MHz. The communications system can transmit and receive signals through low-gain and high-gain antennas. The receiver tracking threshold is a nominal  $-150$  dbm based upon a phase-lock loop noise bandwidth of 20 Hz, and a maximum transponder noise figure of 11 db.

The maximum tolerable spurious noise at the input to the spacecraft's receiver is  $-174.23$  dbm in a 1 Hz bandwidth. It was determined that the Noise Receiver System was capable of measurements as low as  $-151$  dbm in a 100 Hz bandwidth. By use of suitable data reduction, narrower bandwidths with resulting increase in sensitivity could be achieved using frequency conversion and

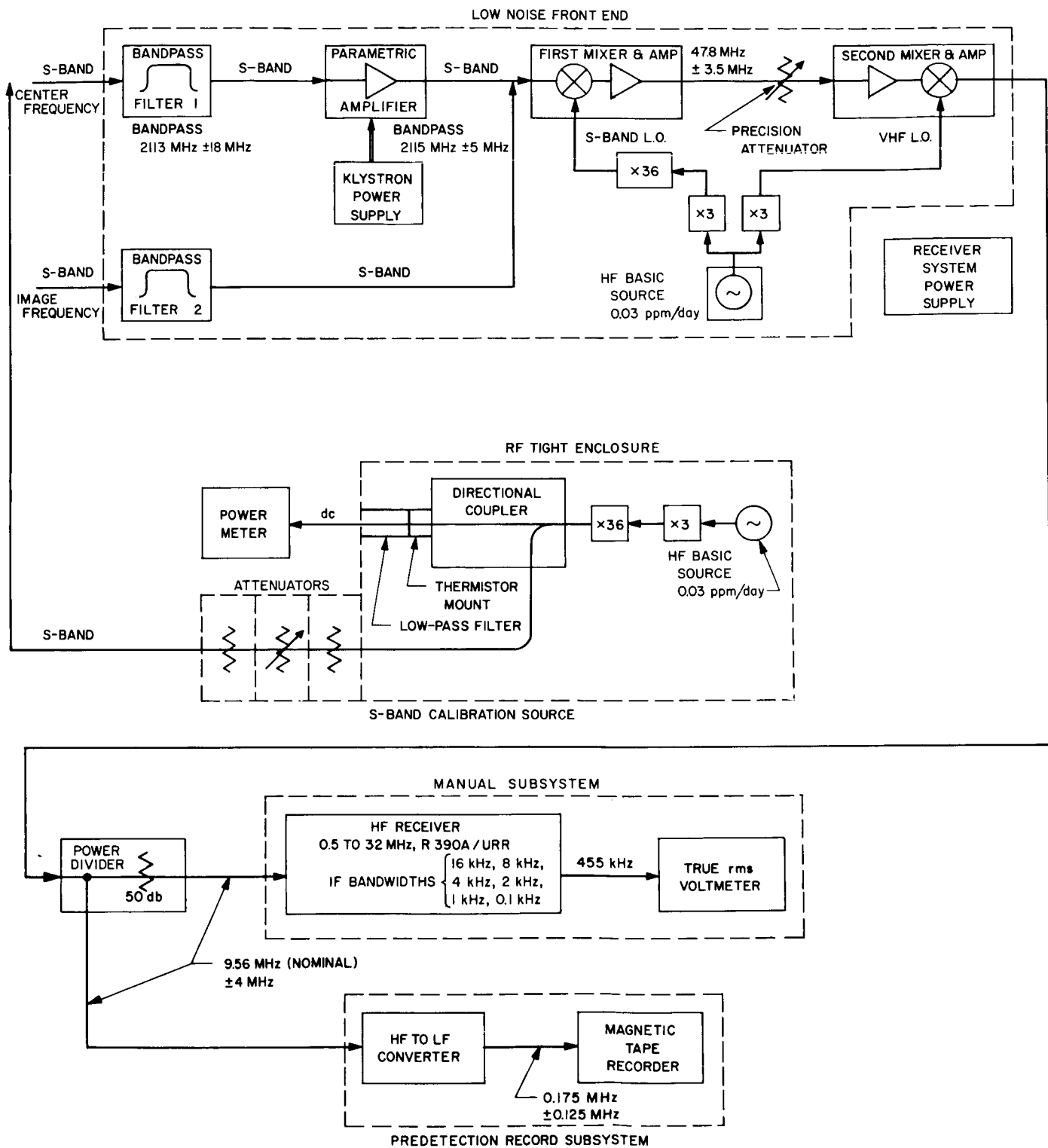


Fig. 1. Functional block diagram S-band Noise Receiver System

magnetic tape recording. This requirement was established as most realistic, consistent with development time and other practical considerations. The basic development task was to provide a readily portable, high resolution, low noise receiver system having a sensitivity approaching that of the permissible noise level for *Mariner* Mars spacecraft, and with a broad tuning range.

### III. System Design

The system design philosophy required the use of proven hardware and designs wherever feasible. Where practicable, the spacecraft transponder design was incorporated to reduce possible differences in system response and to improve the integrity of the measurements. The spacecraft transponder IF frequencies were utilized in the Noise Receiver System front end to obtain the same image frequency rejection response. This approach also allowed the utilization of prototype or non-flight spacecraft transponder modules, resulting in some front-end spare parts capability. An existing military R 390A/URR HF receiver having narrow-bandwidth mechanical filters and accurate frequency readout was incorporated into the system along with a true rms voltmeter. The meter was used as a power indicator at the 455 kHz IF output of the R 390A/URR. To provide the capability of post-test data analysis for the measurement of noise in narrow bands for a relatively wide frequency range, predetection recording was investigated and incorporated into the system. The technique provides an ideal method of applying noise power spectral density computer programs to the analysis. The Noise Receiver System schematic is shown in Fig. 1. For the receiver portion of the system, there were two areas of major effort: (1) the design of a sensitive front-end that would provide a low noise figure, and a frequency conversion from S-band to HF, and (2) the design of a converter that would translate a small band of the HF information to the LF range suitable for predetection recording.

#### A. Receiver Sensitivity Considerations and Front End Design

A design objective was established that the receiver noise figure should not exceed 3 db. This noise figure sets the theoretical system threshold at -151 dbm in a 100 Hz bandwidth. This threshold is based upon the relationship

$$S_T = F k T_o B$$

$$S_T \text{ (dbm)} = F \text{ (db)} + (k T_o B) \text{ dbm}$$

$S_T$  is the receiver threshold

$F$  is the receiver noise factor

$k$  is Boltzmann's constant  
( $1.38 \times 10^{-23}$  watt-sec/°K)

$T_o$  is 290°K

$B$  is the receiver noise bandwidth in Hz

For a bandwidth of 100 Hz and a noise figure of 3 db,  $S_T = -151$  dbm.

For the front end, a low-noise parametric amplifier was used in conjunction with a low-loss preselector and two stages of low-noise conversion. The noise figure,  $F$ (db), calculation is shown below. It is based upon practical noise figures and gains available in state-of-the-art equipment and in the existing equipment. Figure 2 shows a simplified four-stage network of the Fig. 1 cascade system. Given the numeric value of the noise factor ( $F$ ) and gain ( $G$ ) for each stage, the overall noise figure of the Fig. 2 system can be calculated as follows:

$$\begin{aligned} F_a &= 1.58 & F_b &= 10 & F_c &= 10 & F_d &= 31.6 \\ G_a &= 100 & G_b &= 31.6 & G_c &= 1 & & \end{aligned}$$

( $G_c$  was set at 0 db for dynamic range purposes.)

$$\begin{aligned} F &= F_a + \frac{F_b - 1}{G_a} + \frac{F_c - 1}{G_a G_b} + \frac{F_d - 1}{G_a G_b G_c} \\ F &= 1.580 + \frac{9}{1 \times 10^2} + \frac{9}{3.16 \times 10^3} + \frac{30.6}{3.16 \times 10^3} \\ F &= 1.580 + \approx 0.09 + \approx 0.003 + \approx 0.010 \\ F &\approx 1.68 \\ F \text{ (db)} &\approx 2.26 \text{ db} \end{aligned}$$

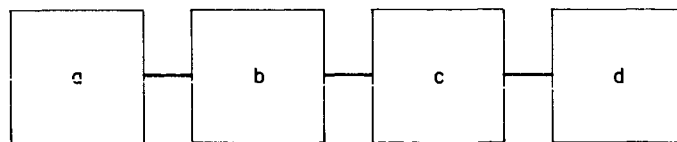


Fig. 2. Four networks in cascade

#### B. System Description

The parametric amplifier (Fig. 1) variable reactance is provided by a varactor diode in conjunction with a klystron pump. The front-end preselector and two mixer amplifier stages are spacecraft flight-type modules used

in the receiver section of the *Mariner Mars 1964* spacecraft transponder. Since the front end contains one oscillator which is high in frequency with respect to the information band, the HF output frequency band is reversed with respect to the input, i.e., the upper frequencies of the original passband appear as the lower frequencies of the converted signal, and vice versa. The mixer local oscillator signals are generated by one stable HF crystal source housed inside a proportionally controlled oven. The signal is frequency multiplied through two multiplier chains prior to the two IF mixers. The triplers are conventional transistorized units. The  $\times 36$  multiplier employs varactor diodes and a highly selective S-band cavity filter. The latter unit is a spacecraft flight-type module used in the receiver section of the *Mariner Mars 1964* spacecraft transponder. A precision IF attenuator is incorporated in the receiver for system noise figure measurements. It can be seen from Fig. 1 that the front end converts a 7 MHz bandwidth of information from S-band to HF; the 7 MHz passband center can be varied several megahertz by changing crystals in the local-oscillator basic source. This capability affords complete coverage of the range 2110 MHz to 2120 MHz.

**1. Manual Scan Subsystem.** The manual scan subsystem provides the real-time capability for high resolution examination of frequency data from the low-noise front

end. The R 390A/URR receiver is tuned through the HF output band, and linear indication of noise, interference, etc., is given by the true rms voltmeter measurement of the R 390A/URR IF output. This examination can be performed in several degrees of detail by using the six IF bandwidths, including 100 Hz available with the R 390A/URR receiver. The true rms voltmeter is a Ballantine model 320. This unit measures the true rms value of complex waveforms with all significant components in the range from 5 Hz to 500 kHz. The output of the R 390A/URR receiver is 455 kHz, extending  $\pm 8$  kHz or less, depending upon which IF bandwidth is used.

**2. Predetection Record Subsystem.** The predetection record subsystem, with the low-noise front end, provides the capability to record a band of data about the S-band frequency of interest. It is an HF-to-LF converter, designed and developed at JPL. Very low levels of data can be recorded on tape and these data can be analyzed in detail at a later date. The LF information which is recorded is a 250 kHz bandwidth centered about 175 kHz; this band corresponds to a 250 kHz bandwidth centered about the S-band frequency of interest. A block diagram of the system is shown in Fig. 3. The HF-to-LF converter consists of two stages of conversion with associated filtering and amplification.

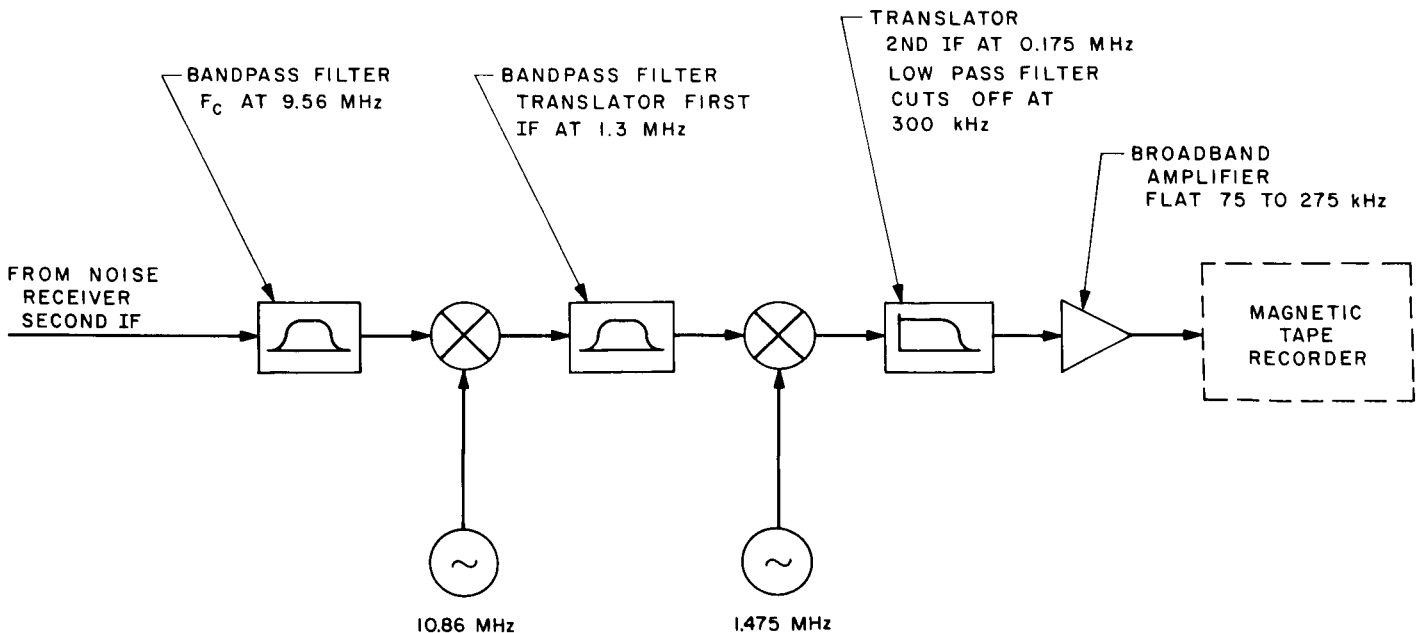


Fig. 3. S-band Noise Receiver System predetection record subsystem

### C. S-Band Calibration Source

In order to measure the Noise Receiver System sensitivity and dynamic range in relatively narrow bandwidths (100 Hz, 1 kHz), it was necessary to develop a sine wave calibration source which generated highly stable S-band signals at continuously variable output levels in the neighborhood of  $-151$  dbm and greater. The block diagram of this calibration source is shown in Fig. 1. The entire calibration source is housed inside an RF-tight enclosure. This design is based on an existing design which was developed for a similar source used to test spacecraft flight transponders. The calibration source consists of a stable HF crystal (housed in a

proportionally controlled oven) and a frequency multiplier chain. The frequency of the source can be adjusted to the accuracy of a laboratory counter that is capable of  $\pm$  one count  $\pm 5$  parts in  $10^8$ . This frequency chain is virtually identical with the local oscillator chain used in the low-noise front end (Section III-A.). The output from the  $\times 36$  multiplier is a stable spectral line of approximately 0 dbm power level.

This power is divided into two channels with a directional coupler. In one channel, a high percentage of the power is dissipated in a thermistor mount which is used for power monitoring and is attached directly to the directional coupler. The output from the thermistor mount is essentially dc with a potentially troublesome component at the S-band frequency. This component is removed by passing the thermistor mount output through a low-pass filter located inside the RF enclosure prior to application to the power meter external to the enclosure. The power which is not dissipated in the power monitor channel is transferred to the calibration source channel. In this channel, the power is attenuated by one variable and two fixed attenuators. The variable attenuator is a PRD model 198 waveguide beyond cutoff attenuator. Each attenuator is housed in a separate compartment within the RF enclosure in order to ensure the integrity of the attenuation chain. The output from the calibration source may be varied over a range of several megahertz by changing the HF crystal in the basic source; the maximum power level is variable (depending upon the fixed attenuation chosen) and has a lower limit set by the noise in a 1 Hz bandwidth at  $290^\circ\text{K}$  (approximately  $-174$  dbm/Hz). Appendix A includes a graph of S-band power output as a function of dial setting for a particular frequency and a set of attenuation components. The physical configuration of the calibration source is shown in Fig. 4.

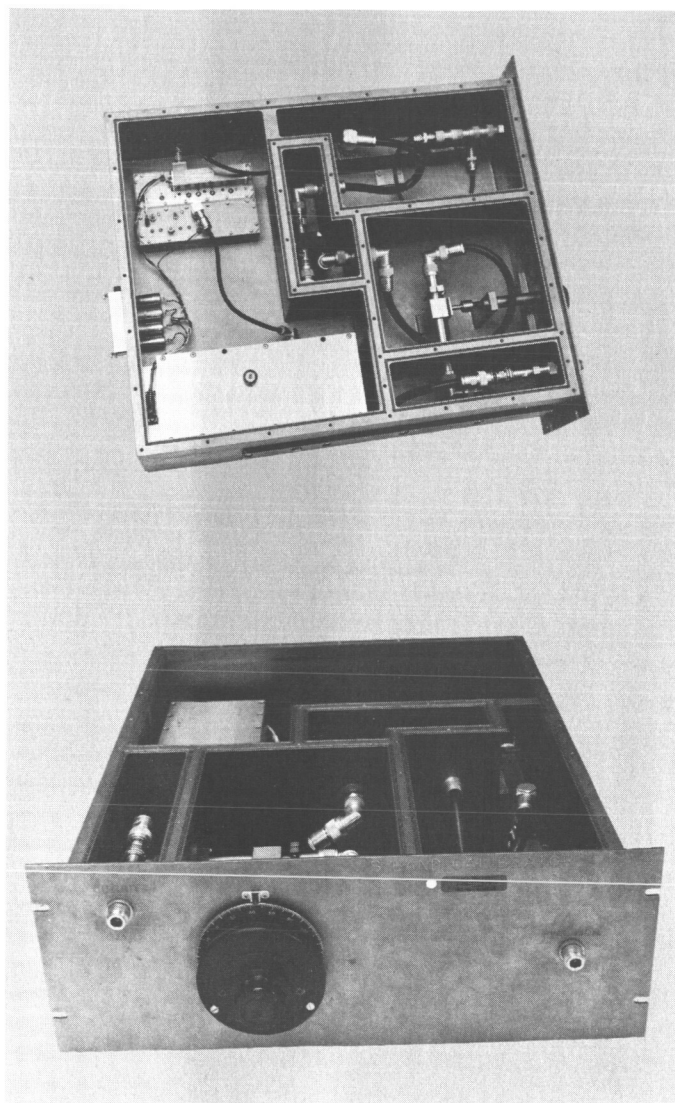
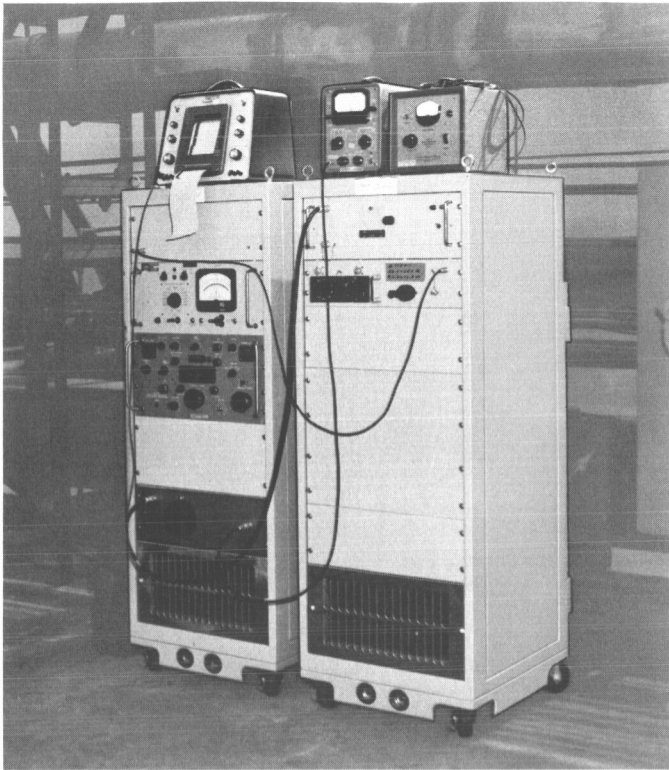


Fig. 4. S-band Noise Receiver System CW calibration source: Top and front views

## IV. System Calibration, Operation, and Performance Capabilities

### A. System Packaging and Calibration

The S-band noise measurement system is housed in 2 five-foot-high portable racks. This configuration, with the calibration source housed in a separate rack from the receiver front end, is used in an effort to ensure measurement integrity. While RF seals are provided by the racks, the racks do have some RF leakage through holes and meter faces on instrument panels. The complete system is shown in Fig. 5. All external cables employ double shields.



**Fig. 5. S-band system packaging in consoles  
(in use at the AFETR)**

The noise figure of the system has been measured (Appendix A). The results show that the system noise figure is approximately 3 db; this value sets the theoretical system threshold at  $-151$  dbm (100 Hz bandwidth) and  $-141$  dbm (1 kHz bandwidth) for an input termination at  $290^{\circ}\text{K}$ . A dynamic range curve for the manual system is shown in Fig. 6. This curve was made for a 1 kHz system bandwidth and indicates that the system 3 db sensitivity for that bandwidth is  $-143$  dbm. The 2 db discrepancy is comparable to the system calibration uncertainty when taking into account the cable and connector attenuation measurement uncertainties, and the S-band calibrator measurement accuracy limitations ( $\pm 1.60$  db to  $\pm 1.20$  db high and low power levels, respectively).

#### **B. System Operation and Performance Capabilities**

The instrumentation is designed for use in normal ambients (nominally  $72^{\circ}\text{F}$ ). Prior to usage, the system is allowed to warm up for at least one hour and the parametric amplifier is calibrated for 20 db insertion gain. After a satisfactory system threshold check by means of the calibrator, the system is ready for use (see Appendix A for this procedure). The mathematical

evaluation of the real-time system performance capabilities and parameters are essentially those given in Ref. 1.

### **V. S-Band Noise Receiver Operations Summary**

While no major compatibility problems were encountered, the S-band Noise Receiver System proved valuable in providing assurance of the compatibility of the spacecraft communications with the operations environment. Specifically the system supported the *Mariner* Mars 1964 Project in the following manner:

1. Verified that undesirable noise levels or spurious spectral components were not present in or close to the spacecraft receiver passband when measured in a simulated space environment.
2. Verified that the passbands for the several allocated receiver frequencies were free of interference at the launch complex at Cape Kennedy.
3. Provided a versatile sensitive receiver on a standby-basis during crucial tests at Pasadena and Cape Kennedy.

The Noise Receiver System performed reliably and accurately in tests at Pasadena and Cape Kennedy. Except for an incident that has not been completely explained in which the klystron power supply of the parametric amplifier failed in Pasadena, no other equipment malfunctioned. At Cape Kennedy, the tests were essentially conducted in the high humidity and temperature of the launch complex ambient. That environment did not adversely affect the receiver equipment. Descriptions of the Noise Receiver tests during *Mariner* spacecraft test operations at JPL, Pasadena and at AFETR, Cape Kennedy are included in this section of the report.

#### **A. Pasadena Operations Summary**

As indicated in other sections of this report, one of the objectives was that the Noise Receiver be assembled in a relatively short period of time and that the probability of immediate successful operation be high. Throughout the assembly of the Noise Receiver System, the operational use of the unit was kept in mind. Primary design consideration was that trouble-free operation in other than an ideal laboratory environment be assured. As the assembly of the unit proceeded, suggestions that would permit easier operation were incorporated in its design.

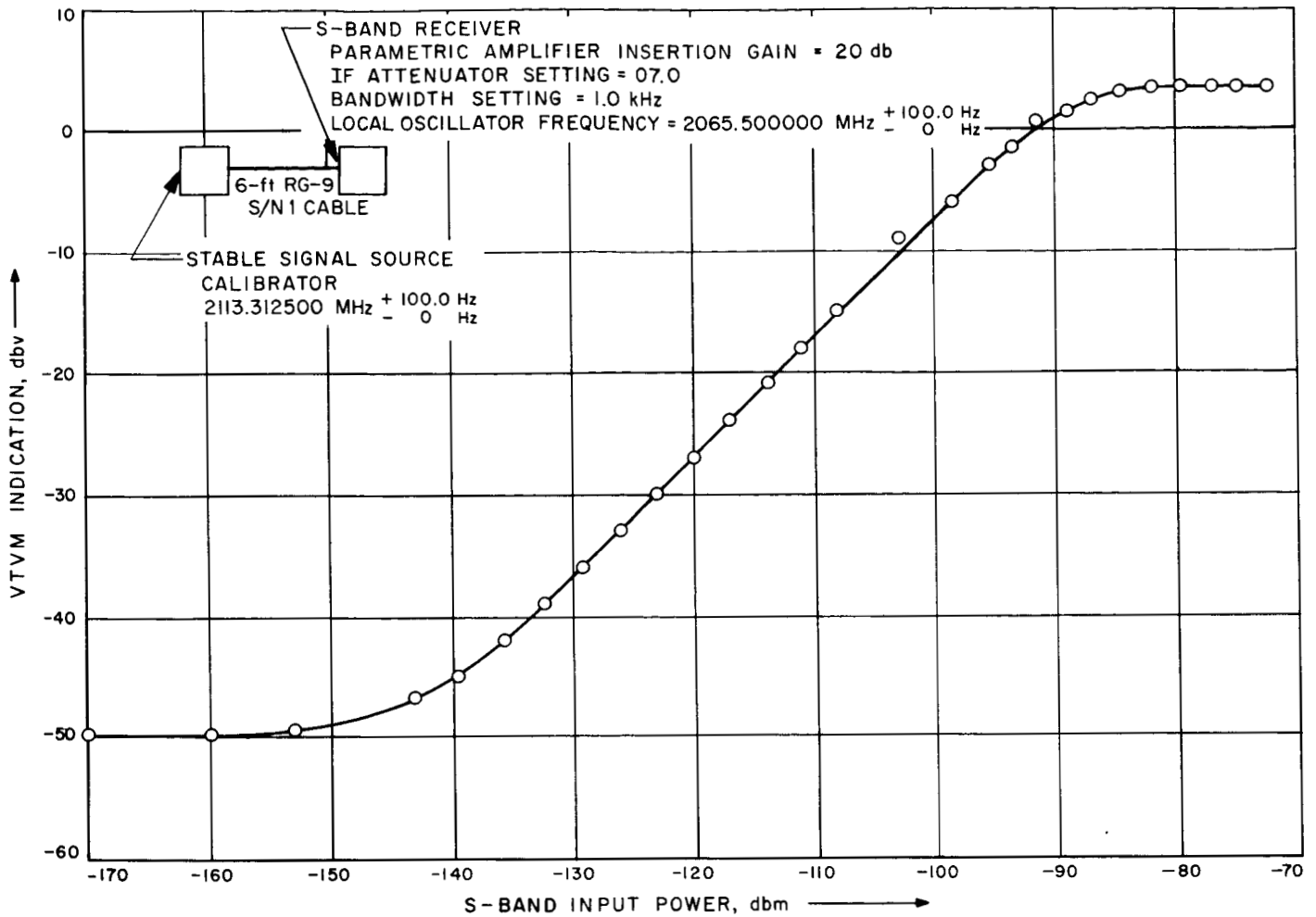


Fig. 6. S-band Noise Receiver System input-output characteristic (manual system)

After bench test of the receiver assembly, the equipment was temporarily installed in a console for use in spacecraft tests. This unit was placed in immediate use to familiarize personnel with the system operational characteristics and determine equipment modifications necessary to adequately support the project requirements.

The equipment was used in space-simulation chamber tests of *Mariner* spacecraft. These tests were made to determine that the spacecraft communications system would not be degraded by broadband RF noise in at least a 100 Hz bandwidth generated by any spacecraft subsystem in a simulated space environment. The noise receiver was connected to the omnidirectional antenna of the *Mariner C* (*Mariner Mars 1964*) spacecraft with low-loss coaxial cables that passed through the space chamber's interface walls. Figures 7 through 9 describe the cable connections.

**1. Noise Receiver Calibration.** To verify that the receiver system was operating properly, three matched terminations at different temperatures were used on the parametric amplifier input, since the CW calibrator had not been finished. These terminations were: (1) a 50-ohm load at ambient temperature, (2) a 50-ohm load immersed in liquid nitrogen, and (3) a gas tube noise source. Magnetic tape recordings were made at various times during the test period and the various terminations were used to provide known levels of noise. The intent was to bracket any noise observed with the ambient termination and the gas tube noise levels.

**2. Test Results.** As a result of noise monitoring during the proof test model (PTM) spacecraft tests, it was discovered that when the attitude control gas jets and the gyros were actuated, a noise was observed in the receiver passband for a short period. The indication

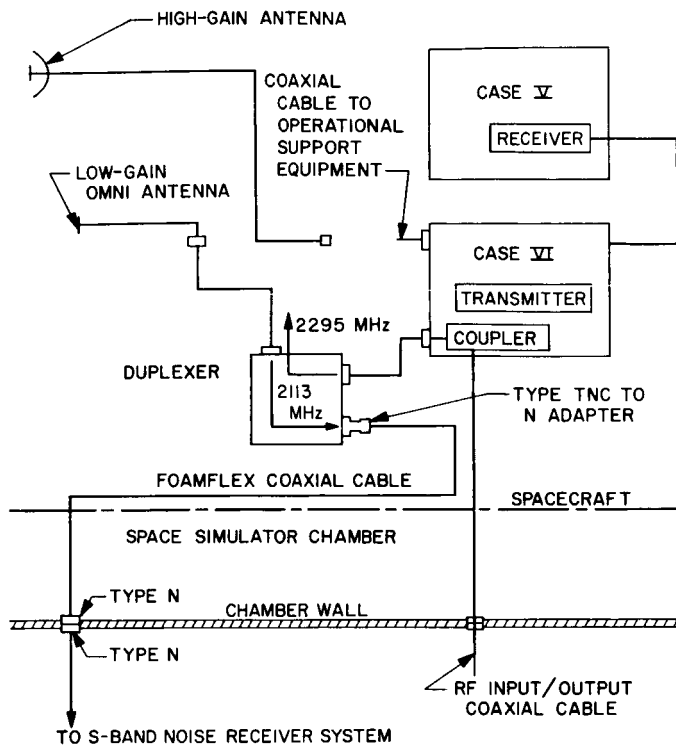


**Fig. 7. EMI test equipment installation on MC-1, proof test model**

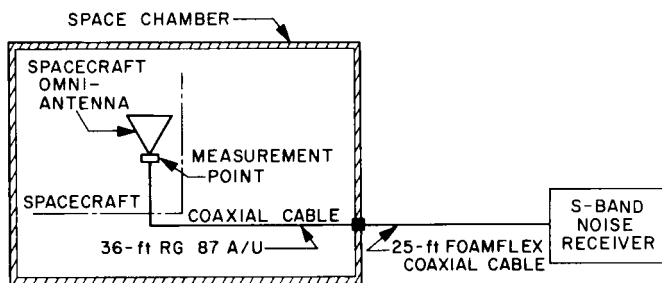


**Fig. 8. Functional diagram: MC-2 mission test**

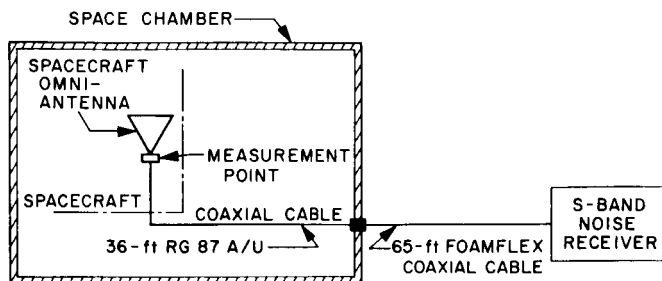


**Fig. 9. Functional diagram: MC-3 and MC-4 mission tests**

appeared as a noise "burst". A recording of this noise was made with the predetection equipment and the magnetic tape was analyzed later. It was determined that the greatest noise burst lasted for approximately 50 msec. It had the approximate amplitude of the gas tube noise source—approximately  $-139$  dbm in 100 Hz—referred to the receiver system input. The results of this measurement were made known to cognizant spacecraft system personnel. It was apparent that operation of the attitude control system on the flight spacecraft should be carefully monitored. Subsequently, similar monitoring tests were performed on the flight spacecraft but the noise bursts were not observed again. Non-repeating, short-duration noise was observed on the first and second flight spacecraft but was outside of the spacecraft receiver passbands.

A special test was performed before Mars encounter on the PTM in the Spacecraft Assembly Facility to investigate the noise bursts. Short coaxial cables allowed an improvement in receiver system sensitivity over that in space simulator chamber tests. An analysis comparing the Noise Receiver's operating sensitivity in the space simulator and the Spacecraft Assembly Facility is included in Appendix B. The test objective was to examine the noise "burst" generation on the PTM spacecraft and attempt to devise methods of "living" with the noise. The noise was not observed; apparently the different configuration or some hardware change had eliminated it. During the spacecraft encounter with Mars, and on other portions of the flight, no anomalous operations which could be attributed to noise bursts were reported.

**3. Preparation for Cape Kennedy Tests.** To prepare the receiver for some tests proposed for the AFETR launch complexes, the Noise Receiver System was returned to the JPL Electromagnetic Interference (EMI) laboratory. During the spacecraft testing period, several design changes had been studied and these were now incorporated. One of these changes was a repackaging of the parametric amplifier that placed controls for the unit on a panel accessible from the front of the console. Another change was an improved layout for the coaxial cable input connectors. The JPL-designed CW calibrator was added to the system. The entire system was installed in two RF-shielded, specially constructed consoles. Each console was short enough and small enough to be easily maneuvered in crowded areas. On a trip to the launch complexes at the AFETR, the service towers and the general area where the S-band noise survey was contemplated were examined by EMI Group



personnel, with the conclusion that any equipment used should be of small physical size. Suitcase-type construction had been considered but was abandoned in favor of the more standard console design.

## **B. Cape Kennedy Operations Summary**

AFETR S-band noise surveys were necessary since the *Mariner* Mars 1964 spacecraft launch was the first JPL spacecraft mission having an S-band transponder system. The S-band noise level in the launch area and the possible effects of such noise on the spacecraft communications were unknown. Unexpected S-band noise could degrade the prelaunch checks and cause costly delays to the project.

**1. Launch-Complex No. 13 Test Configuration and Results.** The RF path for the checkout of the spacecraft omni antenna link was through a parabolic antenna on service deck no. 12 of the service tower. The parabolic antenna was connected to the spacecraft omni antenna by means of a coaxial cable to a parasitic antenna on the spacecraft shroud. The parasitic antenna was coupled through a cable internal to the spacecraft shroud connecting to the spacecraft omni antenna coupler.

The S-band Noise Receiver System was taken to service tower deck no. 13 close to the RF-link parabolic antenna. The coaxial cable was disconnected at the parabolic antenna and a short, low-loss cable was then used to connect the Noise Receiver System to the parabolic antenna. The normal spacecraft operational checkout configuration with the much longer cable-run had a greater signal loss than that of the short cable configuration used with the S-band Noise Receiver System. Consequently, the sensitivity of the S-band Noise Receiver System was appreciably greater than that of the spacecraft receiver system. Each of the five receiver frequencies allotted for the *Mariner* Mars 1964 Project was monitored for noise levels at various times during several days.

The RF path for the checkout of the spacecraft high gain antenna link was through a parabolic antenna on the umbilical tower. Operationally, the antenna was connected by cable through the umbilical connector to a power monitor at the spacecraft high gain antenna. For this portion of the tests, the S-band Noise Receiver System was placed at the base of the umbilical tower. A low-loss coaxial cable was extended from the antenna down to the receiver. A test similar to the one described above was performed with the umbilical tower parabolic

antenna. In addition to the operational parabolic antennas that were employed for the survey, a portable S-band horn antenna mounted on a tripod was used to observe noise from various directions. The purpose of the test was to observe noise that could leak into the system. No S-band noise was observed during the test periods.

During some on-pad tests (Combined System Test) of the spacecraft, launch vehicle and AFETR launch environment, the noise receiver equipment was transferred to the base of the umbilical tower and a horn antenna at the top of that tower was used to monitor the noise level. No interference from either noise or spurious signals was reported by the spacecraft telecommunications cognizant personnel, nor was any interference detected by the Noise Receiver System. An objective of placing the noise receiver at the base of the tower during spacecraft-launch vehicle checkouts was to have a separate versatile receiver available to track down and identify potential interfering signals. This standby support was requested by the Spacecraft Operations Manager.

**2. Launch-Complex No. 12 Test Configuration and Results.** On launch-complex no. 12, the noise levels were monitored with the noise receiver at the base of the umbilical tower connected to a horn antenna on the umbilical tower. No noise was observed.

**3. Receiver System Calibration at Cape Kennedy.** Calibration of the S-band Noise Receiver System at Cape Kennedy was performed with the CW calibrator. At Pasadena a chart had been prepared showing the calibration attenuator position vs the power level output (Appendix A, Fig. A-1). In calibrating and checking the receiver, the calibrator signal was connected to the parametric amplifier input and varied in amplitude until the background noise level was exceeded by 3 db on the VTVM. The signal level required for this 3 db displacement then provided the receiver system sensitivity directly. Throughout the test period, the sensitivity was frequently checked and it was found to vary not more than a fraction of a db. The CW source frequency stable oscillator was used to accurately tune the noise receiver.

No predetection recording was performed at Cape Kennedy but some recording of the R 390A/URR receiver diode load output was made with a low-speed strip chart recorder. The recording was made as an aid in monitoring to decrease operator fatigue during the

VTVM observation. The strip chart was easily calibrated with the CW stable source.

## **VI. System Design Improvements for Future Operational Requirements**

### **A. Tunnel-Diode Amplifier**

In order to connect the receiver to the measurement point on the spacecraft for the mission test in the vacuum chamber, a 100-ft cable is required. This cable has considerable loss, which degrades the system sensitivity accordingly. One method of improving the system sensitivity in this case (or any case involving long input cables) is to operate a tunnel diode amplifier (TDA) remotely at the measurement point. The TDA can be operated remotely because it requires low level dc power, which is readily available from small dry-cell

batteries, and does not require operating adjustments. A 6.5 db system sensitivity improvement has been calculated for one such configuration.

### **B. Military Receiver R 390A/URR Motor-Driven Scan**

The initial system design for the S-band Noise Receiver called for the R 390A/URR receiver to be tuned manually through the HF band. This method provides no measurement record and is a very monotonous process for the operator. A solution to this problem is to motorize the receiver scan mechanism, and operate an X-Y recorder with the motor and the Ballantine VTVM. The Ballantine VTVM provides a dc voltage which is proportional to the rms value of its input voltage. This scan method will remove the operator manual scan requirement and will provide a real-time frequency vs power measurement record.

## Appendix A

### Receiver System Noise Figure Measurements and Operation Procedure

#### I. Sensitivity Measurement

As a measure of the sensitivity, the noise figure of the Noise Receiver was periodically checked, using the two methods described below. The first method, with a CW source, is better for quick measurement. As mentioned in the operations sections of this report, the first method was used primarily at Cape Kennedy during the launch complex noise surveys. The second method has been in use since the initial calibrations of the Noise Receiver System.

**Method I:** A calibrated CW signal source is applied to the input of the Noise Receiver, and the output of the 9.56 MHz IF amplifier is displayed on an indicator. The indicator for these measurements has been the Noise Receiver System equipment to which the 9.56 MHz IF is connected. This indicator includes the R 390A/URR receiver with its known bandpass filters. With a 50-ohm

matched termination at the receiver input, the indicator reading is proportional to the total output noise power. This power is composed of an increment from the source impedance and one from the noise contributed by the receiver. After the noise level is determined, the signal generator is connected and adjusted to cause an indication twice the value seen before. (Alternately, the IF attenuator can be increased to lower the displacement to the previous level to eliminate any nonlinearity of the indicator portion of the receiver.) Under this condition, the signal-to-noise power ratio is unity and the calibrator power level is read from the CW calibrator (Fig. A-1). The sensitivity for the particular bandpass setting on the R 390A/URR is then defined as that CW power level that will displace the previous reading by 3 db.

**Method II:** In the second method the noise figure is measured using a known source of broadband noise power

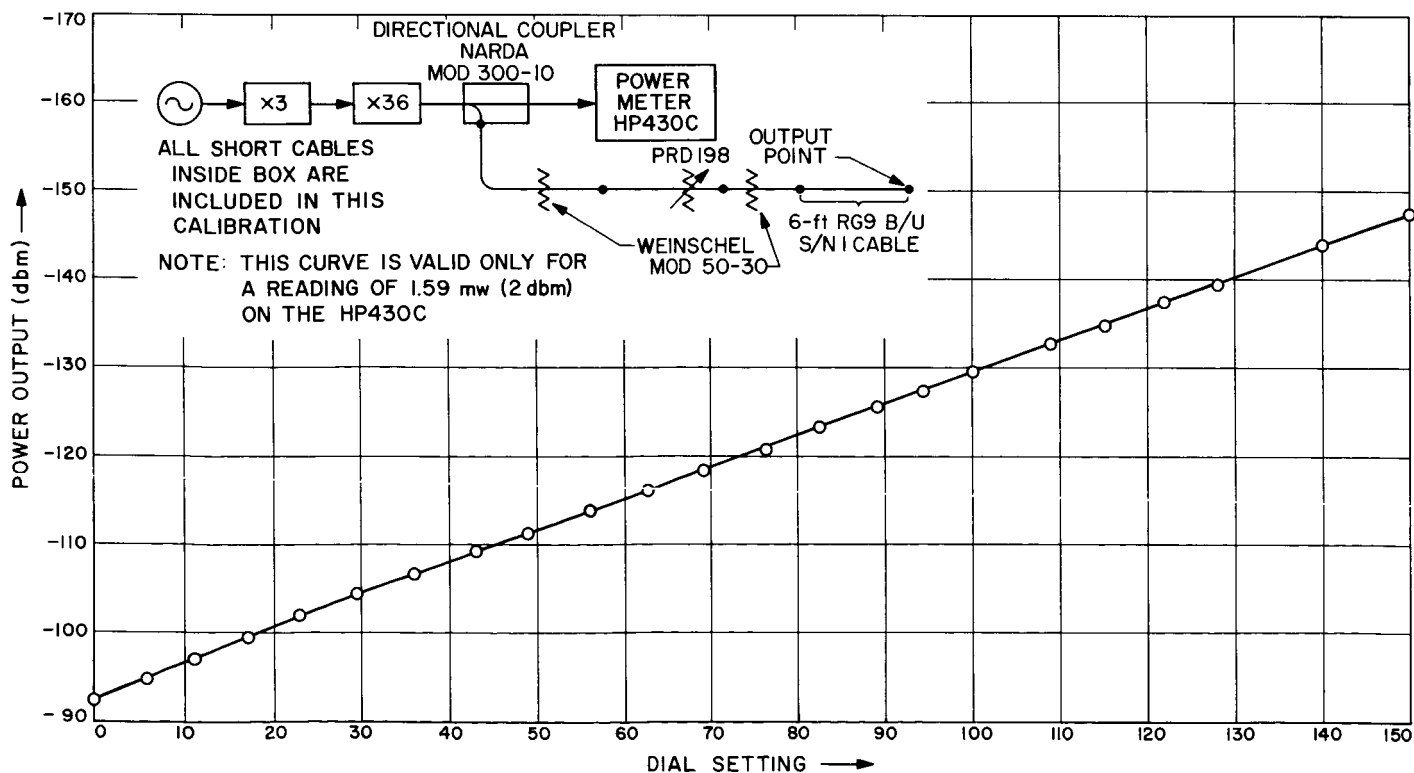


**Fig. A-1. S-band Noise Receiver System calibrator power output curve**

such as an argon gas noise tube or a liquid-nitrogen-cooled termination. The noise factor is found by measuring first the noise power output  $N_1$  of the Noise Receiver when a matched ambient-temperature termination at temperature  $T_1$  is connected at the receiver input. In the second step the noise power output is  $N_2$  when a matched known source at temperature  $T_2$  is connected to the receiver input. The temperature  $T_2$  is the equivalent temperature of a resistance at the receiver input that would produce the same noise power as the known noise source. An expression for noise figure using the known temperature values can then be used.

Noise figure measurements were made by the second method using the configuration of Fig. A-2. The procedure of one measurement is:

$$\text{Noise factor} = F = \frac{(T_2/T_0) - 1}{Y - 1} \frac{B_o}{B} - Y \frac{(T_1/T_0) - 1}{Y - 1} \frac{B_o}{B}$$

(per Ref. 2)

$B_o$  is the total bandwidth of the receiver;

$B$  is the useful bandwidth of the receiver;

$T_0$  is the temperature of a matched input termination at 290°K;

$T_1$  is the temperature of a matched input termination at ambient;

$T_2$  is the noise generator temperature ( $10.1 \times 10^3$ °K for the argon gas tube used)

$Y$  is the ratio  $P_2/P_1$  where  $P_2$  and  $P_1$  are the Noise Receiver power outputs associated with the two terminations.

For this measurement  $B_o/B = 1$ . This reduces the above equation to

$$F = \frac{[(T_2/T_0) - 1] - Y [(T_1/T_0) - 1]}{Y - 1}$$

The  $Y$  factor was measured to be 12.5 db (17.8 numeric) by using the variable IF attenuator in the Noise Receiver.

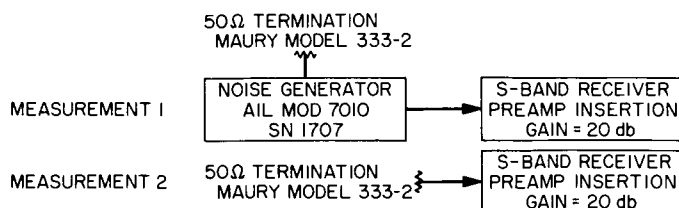


Fig. A-2. Noise figure measurement using Method II

Therefore:

$$F = \frac{\left( \frac{10.1 \times 10^3 \text{°K}}{2.9 \times 10^2 \text{°K}} - 1 \right) - 17.8 \left( \frac{296 \text{°K}}{290 \text{°K}} - 1 \right)}{17.8 - 1}$$

$$F = \frac{33.80 - 0.36}{16.8} = 1.99$$

$$F(\text{db}) = 10 \log_{10} (1.99) \approx 3 \text{ db}$$

Noise figure measurements were also made with the aid of a liquid-nitrogen-cooled termination. The results were essentially the same, indicating good linearity of the system for the noise power range of both sources. For future measurements, a suitable attenuator should be inserted at the gas tube output to minimize impedance mismatch with the gas tube on or off.

## II. Frequency Stability

The design of the oscillators used in the Noise Receiver local oscillator and in the CW calibrated generator has been described in this report. It has been verified by laboratory tests that the oscillators are stable.

## III. Parametric Amplifier Adjustments

Frequency and gain adjustments are made on the parametric amplifier after the proper warmup periods have been allotted.

### A. Frequency Peaking

1. Connect the CW calibrator signal to the parametric amplifier.
2. With a low level signal (approximately -90 dbm), adjust the frequency control for a maximum displacement of the VTVM (the R 390A/URR 455 kHz IF level). (One milliwatt is equal to 0 dbm.)

3. Adjust the calibrator power level to prevent off-scale excursion during frequency peaking.

#### **B. Gain Adjustment**

1. Turn the B+ voltage of the parametric amplifier off and set the power level of the CW calibrator at approximately -100 dbm with the R-390 set at a bandpass of 1.0 kHz.
2. Tune the R-390 to obtain the signal and note the level of the 455 kHz IF output on the VTVM or on an oscilloscope.
3. Decrease the level by 20 db to -120 dbm.
4. Turn the B+ on and adjust the attenuator control on the parametric amplifier to display the original indication displayed in step 2.
5. The parametric amplifier is now adjusted for an insertion gain of 20 db. The loss through the parametric amplifier has been measured as 2 db. A gain of 20 db has shown to be a setting that does not cause instability.

An alternate method used to adjust the parametric amplifier gain was utilized before the calibrator was completed. This method employed a standard labora-

tory signal generator that had a pulse modulation function. The S-band RF signal at the parametric amplifier output was connected directly to a crystal detector. The detected output with the parametric amplifier off was displayed on an oscilloscope. Then with the parametric amplifier on, the input signal was adjusted to obtain the previous reading. (It is planned to add a modulator to the calibrator in order to set the gain with a crystal detector mounted at the 47.8 MHz IF output.)

#### **IV. R 390A/URR Receiver Adjustments**

Various applicable calibrations (such as the frequency readout setting) are fully described in the military manual for this receiver. These calibrations were periodically performed on the unit.

#### **V. Calibration of Accessory Equipment**

Other equipments that comprise the Noise Receiver System, such as the VTVM and coaxial cables, are periodically calibrated and inspected. All cables were calibrated for loss using a Weinschel Engineering dual channel insertion loss test set at ambient temperature ( $\approx 294^\circ\text{K}$ ). The minor variation in cable losses vs temperature have been neglected.

## Appendix B

### System Noise Temperature Analysis for Space Chamber Tests and High Bay Tests

#### I. Purpose

The purpose of this appendix is to analyze and compare the system noise temperatures for S-band noise measurements in the space chamber environment and in the Spacecraft Assembly Facility (SAF) high bay environment. The approach used is to determine the noise temperature at the output of each test configuration and compare the resulting sensitivity for each case.

#### II. Space Chamber Configuration Noise Background Tests

The available location for the Noise Receiver required that long lengths of coaxial transmission lines be used. The configuration that would be required in a space chamber test is shown in Fig. B-1.

The noise figure of the S-band Noise Receiver with respect to the input has been measured to be 3 db. This noise figure corresponds to an effective input temperature ( $T_R$ ) of 290°K. The spacecraft antenna output temperature is found as follows. The chamber walls are kept at 105°K during testing; these walls essentially surround

the omni antenna. It is assumed for this analysis that the antenna aperture is illuminated by the walls at 105°K. Time limitations imposed by a tight test schedule did not permit extensive measurements of the impedance match at the spacecraft omni antenna terminals in the space chamber. This analysis assumes a good antenna match. For this condition the antenna temperature is also 105°K ( $T_A = 105^\circ\text{K}$ ) (Ref. 3). This temperature is affected by the losses and temperatures of the connecting antenna mast, coaxial cables, and duplexer. When an antenna at temperature  $T_A$  is connected with a coaxial cable of temperature  $T_c$  and loss  $L_c$  (numeric) to a receiver, the effective input temperature is:

$$T'_A = \frac{T_c(L_c - 1) + T_A}{L_c}$$

The configuration for the simulator chamber has transmission lines at three different temperatures. The equivalent input temperature at the receiver will be determined by three successive calculations. Each calculation will be performed at corresponding temperatures and transmission losses.

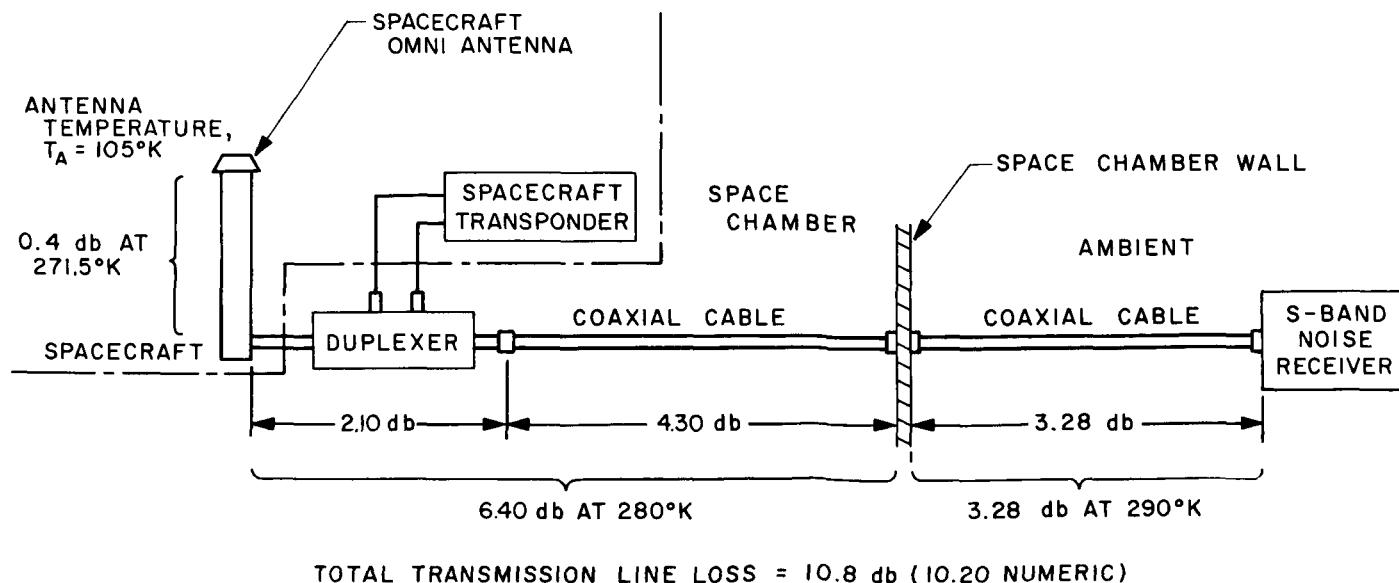


**Fig. B-1. Space chamber test configuration**

At the base of the antenna mast with  $T_c = 271.5^\circ\text{K}$ , the temperature is:

$$T'_A = \frac{271.5^\circ\text{K} (1.097 - 1) + 105^\circ\text{K}}{1.097}$$

$$= 119.7^\circ\text{K}$$

At the simulator chamber interface with the corresponding  $T_c$  now  $280^\circ\text{K}$ , the temperature at the coaxial terminals is:

$$T'_{A_2} = \frac{280^\circ\text{K} (4.365 - 1) + 119.7^\circ\text{K}}{4.365}$$

$$= 243.5^\circ\text{K}$$

Finally, at the S-band Noise Receiver input terminals the temperature is:

$$T'_{A_3} = \frac{290^\circ\text{K} (2.1 - 1) + 243.5^\circ\text{K}}{2.1}$$

$$= 268^\circ\text{K}$$

The effective noise background against which the "signal" competes is then at a temperature equal to the sum of the antenna temperature referred to the receiver input and the effective receiver input temperature

of  $290^\circ\text{K}$  ( $T_R$ ). The temperature of the noise background is:

$$T_{NB_1} = T'_{A_3} + T_R$$

$$= 268^\circ\text{K} + 290^\circ\text{K}$$

$$T_{NB_1} = 558^\circ\text{K} \text{ simulator chamber tests}$$

### III. Spacecraft Assembly Facility High Bay Configuration Noise Background Tests

The configuration available for tests in the SAF high bay permitted shorter lengths of coaxial cables to be used. The spacecraft omni antenna temperature was found to be  $450^\circ\text{K}$  (due primarily to the fluorescent lights in the building) by the method described in Section V below. Although the antenna temperature was  $345^\circ\text{K}$  greater than for the simulation chamber, this configuration with shorter cables and corresponding lower transmission losses yielded an overall noise background temperature comparable to the chamber test. The high bay configuration is shown in Fig. B-2.

The spacecraft omni antenna temperature was determined to be  $450^\circ\text{K}$  by the method discussed in Section V. This antenna temperature would appear at the receiver input as:

$$T'_{A_4} = \frac{290^\circ\text{K} (2.34 - 1) + 450^\circ\text{K}}{2.34}$$

$$= 358^\circ\text{K}$$

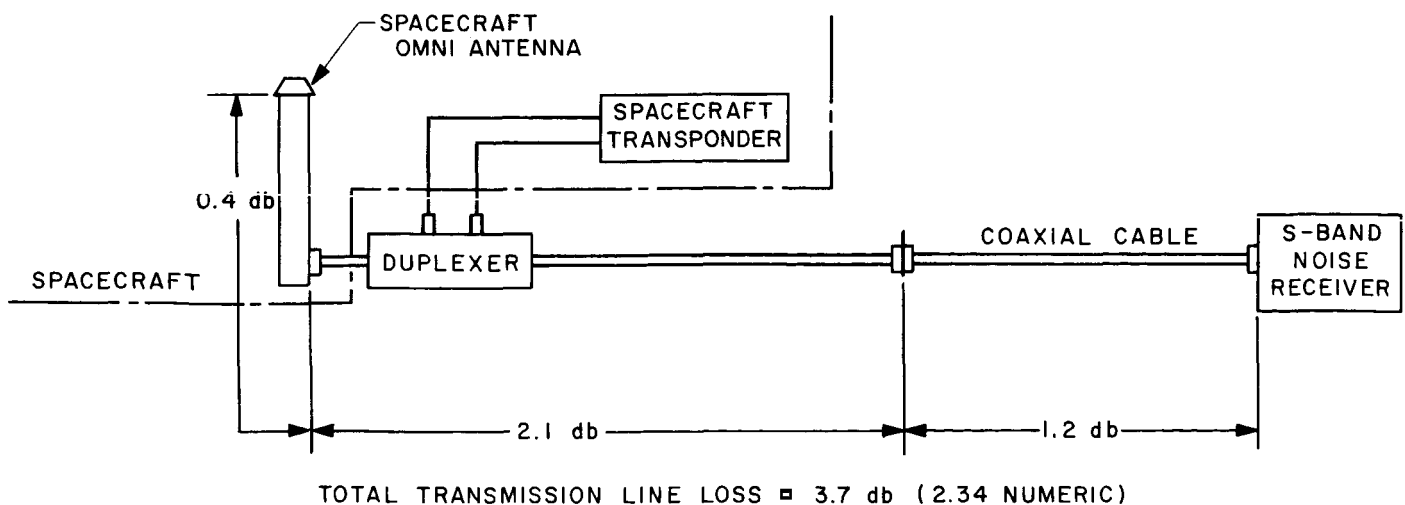


Fig. B-2. Spacecraft Assembly Facility test configuration

The temperature of the noise background against which a "signal" would compete is:

$$\begin{aligned} T_{NB_2} &= T'_{A_4} + T_R \\ &= 358^\circ\text{K} + 290^\circ\text{K} \\ T_{NB_2} &= 648^\circ\text{K high bay tests} \end{aligned}$$

#### IV. System Temperature Comparison

The results of the preceding analysis are as follows:

$$T_{NB_1} = 558^\circ\text{K (simulator chamber configuration)}$$

$$T_{NB_2} = 648^\circ\text{K (SAF high bay configuration)}$$

The improvement in background noise level in the space chamber configuration over the high bay configuration would be the ratio of the two noise temperatures listed above:

In decibels:

$$10 \log \frac{T_{NB}}{T_{NB_1}} = 10 \log \frac{648^\circ\text{K}}{558^\circ\text{K}} = 10 \log 1.16 = 0.64 \text{ db}$$

The sensitivity for each configuration, however, depends on the losses in the cables in addition to the background noise levels. The signal-to-noise ratio for the space chamber simulator configuration is:

$$\frac{S_i}{kT_{NB_1}B}$$

where  $S_i$  is the signal level in watts at the receiver input.

$k$  is Boltzmann's constant ( $1.38 \times 10^{-23} \text{ J}/^\circ\text{K}$ )

$T_{NB_1}$  is the background noise temperature for the space simulator configuration

$B$  is the noise bandwidth of the S-band noise receiver, in Hz

If the signal level at the antenna terminals is  $S$  watts and the loss in the transmission line to the receiver is 10.08 db (10.20 numeric) then:

$$S_i = \frac{S}{10.20}$$

For the space chamber configuration this becomes:

$$\left( \frac{S}{10.20} \right) \frac{1}{kT_{NB_1}B}$$

The signal-to-noise ratio at the Noise Receiver input for the high bay configuration is:

$$\frac{S'_i}{kT_{NB_2}B}$$

where  $S'_i$  is the signal level in watts at the Noise Receiver input.

$k$  is Boltzmann's constant

$T_{NB_2}$  is the background noise temperature for the high bay

$B$  is the noise bandwidth of the Noise Receiver

If the signal level at the antenna terminals is again  $S$  watts and the loss in the transmission line to the receiver is 3.7 db (2.34 numeric) then:

$$S'_i = \frac{S}{2.34}$$

and

$$\frac{S'_i}{kT_{NB_2}B} = \left( \frac{S}{2.34} \right) \left( \frac{1}{kT_{NB_2}B} \right)$$

Since  $T_{NB_2} = 1.16 T_{NB_1}$ ,

$$\frac{S'_i}{kT_{NB_2}B} = \frac{S}{2.34 (1.16 kT_{NB_1}B)} = \frac{S}{2.72 kT_{NB_1}B}$$

The improvement of the signal-to-noise ratio of the high bay configuration over the space simulator configuration is given by  $I$  (db):

$$\begin{aligned} I \text{ (db)} &= 10 \log \left( \frac{\frac{S}{2.72 kT_{NB_1}B}}{\frac{S}{10.20 kT_{NB_1}B}} \right) \\ &= 10 \log \left( \frac{10.20}{2.72} \right) \\ &= 10 \log 3.75 \end{aligned}$$



$I$  (db) = 5.74 db improvement of high bay configuration over space simulator configuration

### V. High Bay Omni Antenna Noise Temperature Measurement

During *Mariner Mars 1964* PTM testing on 20 April 1965, a special test was run to determine the spacecraft omni antenna noise temperature to be expected in the Spacecraft Assembly Facility (SAF) high bay. In the high bay the omni antenna is surrounded by the building walls, floor, and ceiling which are essentially at 300°K. This indicates that the omni antenna noise temperature should also be approximately 300°K (Refs. 3 and 4) in the absence of other temperature sources (lights, etc.). The measurement configuration shown in Fig. B-3 was performed as follows: The spacecraft was located in the test area in the northwest corner of the high bay. All the ceiling lights normally used were on. The omni antenna was connected to the S-band receiver as shown in Fig. B-3. A reading was taken on the Noise Receiver System Ballantine VTVM (the predetection record system was used for this measurement because its relatively large bandwidth affords better noise averaging, hence steady voltmeter needle indications). The omni antenna and cables were then disconnected and a 50-ohm termination (Maury model 333-2) was connected to the Noise Receiver at point B. A VTVM reading was again taken and this reading was found to be 0.7 db lower

than the first reading (with the antenna and cables). The omni antenna noise temperature is found from these data as follows.

For each of the Noise Receiver termination conditions described, there is a corresponding system input noise temperature  $T_s$  at point B. For the Fig. B-3 configuration,  $T_s = T_{s_1}$

$$T_{s_1} = T_R + T_1$$

where  $T_R$  is the effective input noise temperature of the receiver and  $T_1$  is the termination temperature (due to cables and the antenna).

The quantity of interest is  $T_1$ , because it is directly related to the omni antenna noise temperature.  $T_1$  can be determined if  $T_{s_1}$  and  $T_R$  are known.  $T_R$  is found as follows: The noise figure of the S-band Noise Receiver is 3 db.

$$10 \log_{10} \left[ \frac{T_R}{T_o} + 1 \right] = 3 \text{ db}$$

where  $T_o = 290^\circ\text{K}$

$$\frac{T_R}{T_o} + 1 = 2$$

$$T_R = 290^\circ\text{K}$$

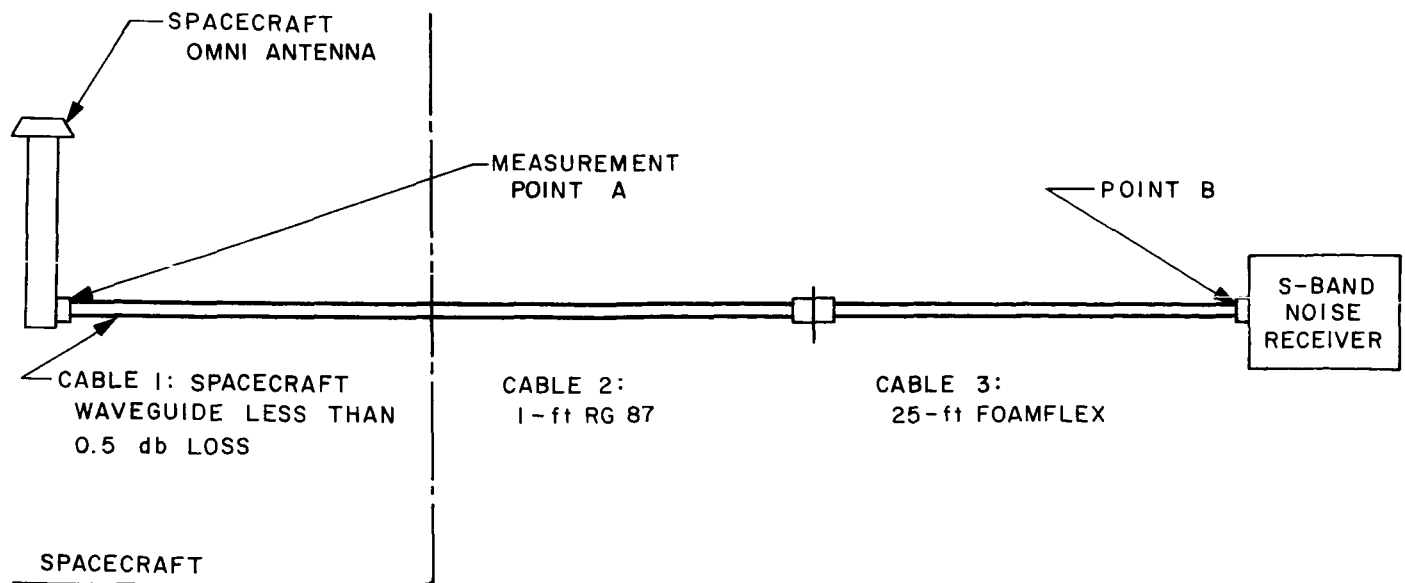


Fig. B-3. High bay omni antenna noise temperature measurement test configuration

$T_{s_1}$  can be found as follows: For the 50 ohm termination case  $T_s = T_{s_2}$

$$T_{s_2} = T_R + T_2$$

where  $T_2$  is the termination temperature (approximately 294°K).

$$T_{s_2} = 290^\circ\text{K} + 294^\circ\text{K}$$

$$T_{s_2} = 584^\circ\text{K}$$

Total system noise output is directly related to the system input noise temperature at point B. Therefore,

$$10 \log_{10} \left[ \frac{T_{s_1}}{T_{s_2}} \right] = 0.7 \text{ db}$$

Where 0.7 db was the difference in indicator readings for the two temperature conditions,

$$\begin{aligned} T_{s_1} &= 1.18 [T_{s_2}] = 1.18 (584^\circ\text{K}) \\ &= 690^\circ\text{K} \end{aligned}$$

Therefore

$$\begin{aligned} T_1 &= T_{s_1} - T_R = 690^\circ\text{K} - 290^\circ\text{K} \\ T_1 &= 400^\circ\text{K} \end{aligned}$$

The noise temperature at point A in Fig. B-3 (the waveguide output) is essentially the same as that of the antenna itself because the waveguide loss is less than 0.5 db. The noise temperature at point A is related to  $T_1$  by the equation

$$T_1 = \frac{290^\circ\text{K} (L - 1) + T_A}{L}$$

where  $L = 1.45$  (1.6 db)

$$T_A = (1.45) (400^\circ\text{K}) - (290^\circ\text{K}) (.45)$$

$$T_A = 580^\circ\text{K} - 130^\circ\text{K}$$

$$T_A = 450^\circ\text{K}$$

This result is of the order of magnitude expected and is somewhat higher than 300°K due to the noise temperature of the ceiling lights subtended by the antenna beamwidth. During this test the high bay lights were turned off and the indicator level decreased. This antenna noise temperature probably will vary slightly for different locations within the high bay but should not vary greatly as long as the antenna is kept relatively near the floor (approximately 10 ft) as in typical test configurations.

## References

1. Biber, K. W., and Whittlesey, A. C., *Description and Analysis of 890-MHz Noise Measuring Equipment*, NASA TR 32-898, National Aeronautics and Space Administration, Washington, D. C., March 1966.
2. Fox, J., and Sucher, M., Editors, *Handbook of Microwave Measurements: Volume III*, Third Edition, p. 875, Polytechnic Press of the Polytechnic Institute of Brooklyn, Brooklyn, N. Y., 1963 (Distributed by Interscience Publishers).
3. Brown, R. H., and Lovell, A. C. B., *The Exploration of Space by Radio*, p. 24, John Wiley & Sons, Inc., New York, N. Y., 1958.
4. Pawsey, J. L., and Bracewell, R. N., *Radio Astronomy*, pp. 21-24, Clarendon Press, Oxford, England, 1955.